Materials Science Forum Vols. 660-661 (2010) pp 209-214
Online available since 2010/Oct/25 at www.scientific.net

doi:10.4028/www.scientific.net/MSF.660-661.209

Investigation on the corrosion resistance of PIM 316L stainless steel in PEM fuel cell simulated environment

Mara Cristina Lopes de Oliveira[1, a], Isolda Costa[2,b] and Renato Altobelli Antunes[3,c]

[1]Electrocell Ind. Com LTDA. - Av. Prof. Lineu Prestes, 2242 – Ed. CIETEC – Cidade Universitária – 05508-000 - São Paulo – SP - Brazil

[2]IPEN – Av. Prof. Lineu Prestes, 2242 – Cidade Universitária - -5508-000 São Paulo – SP - Brazil

[3]UFABC – R. Santa Adélia, 166 – Bangu – 09210-170 – Santo André – SP - Brazil

[a]mara.oliveira@usp.br, [b]icosta@ipen.br, [c]renato.antunes@ufabc.edu.br

Keywords: 316L, powder injection molding, corrosion, PEM fuel cell, bipolar plate

Abstract. Bipolar plates play main functions in PEM fuel cells, accounting for the most part of the weight and cost of these devices. Powder metallurgy may be an interesting manufacturing process of these components owing to the production of large scale, complex near-net shape parts. However, corrosion processes are a major concern due to the increase of the passive film thickness on the metal surface, lowering the power output of the fuel cell. In this work, the corrosion resistance of PIM AISI 316L stainless steel specimens was evaluated in 1M H_2SO_4 + 2 ppm HF solution at room temperature during 30 days of immersion. The electrochemical measurements comprised potentiodynamic polarization and electrochemical impedance spectroscopy. The surface morphology of the specimens was observed before and after the corrosion tests through SEM images. The material presented low corrosion current density suggesting that it is suitable to operate in the PEM fuel cell environment.

Introduction

The fuel cell market for powering vehicles is potentially huge. Even if automakers have not reached mass production due to technical and economical barriers, they continue to invest in demonstration and test marketing programs in fuel cell powered vehicles. This strategy is based upon the need for reducing carbon emissions as a result of increasing environmental legislation constraints. Polymer electrolyte membrane (PEM) fuel cells play a major role in this scenario. These devices generate electricity through a direct chemical reaction between hydrogen and oxygen producing only heat and water as byproducts. A schematic view of a typical PEM fuel cell is shown in Fig. 1. The structure of a PEM fuel cell consists of two components: bipolar plates and the assembly known as MEA (membrane electrode assembly). The MEA is comprised of gas diffusion layer (GDL), polymer electrolyte membrane and the catalyst layer. The bipolar plates are the skeleton of the device owing to its mechanical stability and concentrating the most fraction of its total weight. According to Tsuchyia and Kobayashi [1] this fraction may reach up to 80%. Furthermore, bipolar plates are tightly related to the distribution of fuel (hydrogen) and oxidant (oxygen) in the cell structure, to the management of water and to the electric current flux in the cell. The transport of water and gases is carried out through channels that are machined or directly molded in the bipolar plate, depending on the manufacturing process. Bipolar plate materials must be carefully selected in order to achieve such a vital group of functions.

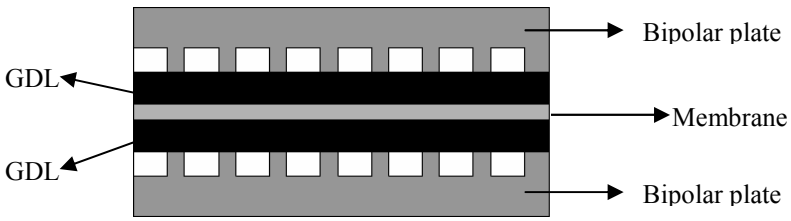

Figure 1. Schematic view of a PEM fuel cell.

The materials traditionally envisaged as bipolar plates are graphite, polymer-graphite composites and metals. Graphite plates have high electrical conductivity but are intrinsically fragile and lack mechanical resistance. Polymer-graphite composites are less prone to mechanical fracture as the

polymer matrix imparts toughness to the composite structure. Nevertheless, as the polymer content increases, the electrical conductivity decreases and the overall current output of the fuel cell may be negatively influenced. So, a careful balance between conductive filler and polymer contents must be determined to achieve an optimum performance. Metal bipolar plates, on the other hand, present excellent mechanical resistance which is a strong advantage for vehicle applications as they can resist eventual shocks and vibrations. Additionally, metals are intrinsic high electrical conducting materials and may be produced in a cost-effective way in a plate shape by means of either stamping or rolling operations.
The PEM fuel cell environment is typically a solution of H_2SO_4 0.5 M with pH 2-4 and small concentrations of HF at a temperature range of 60 to 80 ºC. Metals are prone to corrosion under these conditions. Therefore, metals considered for bipolar plates manufacture must be corrosion-resistant alloys such as stainless steels or aluminum. There are several investigations on wrought stainless steel bipolar plate corrosion in the literature [2-8]. Powder injection molding (PIM) is a manufacturing process that may produce near net shape parts in an economical way. Nevertheless, there are very scarce references on the use of PIM to the manufacturing of PEM fuel cell stainless steel bipolar plates. The aim of this work was to investigate the corrosion resistance of PIM AISI 316L stainless steel in H_2SO_4 0.5 M + 2 ppm HF solution at room temperature in order to establish an initial path towards the suitability of powder metallurgy products as bipolar plates in PEM fuel cells.

Experimental

The material tested in this investigation was gas atomized PIM AISI 316L stainless steel from Steelinject a division of Lupatech S. A. The nominal chemical composition is shown in Table 1. Silveira et al. [9] have characterized the porosity of this material. They found the porosity to be 7.94% with a mean pore size of 3.40 μm.
The corrosion resistance of the specimens was evaluated by means of electrochemical impedance spectroscopy (EIS) and potentiodynamic polarization curves. The specimens were immersed in 0.5 M H_2SO_4 + 2 ppm HF solution at room temperature during 30 days. The evolution of the electrochemical behavior was accompanied with EIS measurements. The spectra were obtained over the frequency range of 100 kHz to 10 mHz, with acquisition of 17 points per decade, at open circuit potential (OCP), with an excitation of 10 mV. The spectra were fitted with the software EQUIVCRT developed by the Boukamp group [9] and the corresponding electrochemical electrical circuits are presented as well as the physical meaning of each element. Anodic polarization curves were obtained at a scanning rate of 1 mV s^{-1} from the OCP up to +1500 mV.

Table 1. Chemical composition of the PIM 316L stainless steel specimens (mass percentage).

C	Si	Mn	Mo	Cr	Ni	other	Fe
0.03	0.8	0.8	2.0-3.0	16-18	10-14	2.0 max.	Bal.

All the electrochemical measurements were performed using an Autolab PGSTAT100 potentiostat/galvanostat with frequency response analyzer (FRA) module for the AC measurements. A conventional three electrode cell was used in these tests. PIM 316L stainless steel specimens were the working electrodes, the counter electrode was a platinum wire, and a saturated calomel electrode was used as reference. Grinding was not applied to the surface of the working electrodes in order to preserve the morphology of the outer parts of the pieces.
Scanning electron microscopy observations were carried out on PIM 316L specimens in the as-received and after polarization conditions.

Results and Discussion

The results of EIS measurements after 1, 2, 7, 14, 21 and 30 days of immersion in 0.5 M H_2SO_4 + 2 ppm HF solution at room temperature are shown in Fig. 2. It is clearly seen that the electrochemical behavior did not present significant changes up to the end of the test. The material's response is highly capacitive through a wide frequency range, indicating a strong resistance to the corrosive effects of the acidic electrolyte. Nyquist plots (Fig. 2a) show that the impedance values increased with immersion time. This result points towards a more protective character of the passive film on the stainless steel surface for longer contact with the electrolyte. Other authors [10-11] have found that the corrosion resistance of powder metallurgy stainless steels tends to diminish for longer immersion periods in acidic solutions. A crevice corrosion mechanism within the intrinsic pores of the material would be the cause of the poorer corrosion resistance. As this behavior was not observed in the present work, it is probable that the low porosity level and small mean pore size after sintering of the PIM 316L specimens have at least partially blocked the access of electrolyte. Furthermore, there is a strong relation between this behavior and the development of a thicker and more protective passive layer on the surface of the alloy. The electrolyte penetration is expected to be rather difficult as the metallic material is continuously exposed to the corrosive environment, developing an adherent and homogeneous oxide film. According to Moral et al. [12] the corrosion kinetics decreases when the porosity of sintered stainless steels diminishes. This is due to an effect of blockage of the electrolyte penetration as a result of the smaller active area. The Bode plots of Fig. 2b show that the phase angles become slightly more negative with time. The spectra reveal the presence of two time constants that are not clearly separated spreading out from the medium (MF) to the low (LF) frequency range. The first time constant may be ascribed to reactions occurring in the surface of the stainless steel, representing the corrosion resistance of the oxide layer. The second one is likely due to the substrate underneath the oxide film. It forms a wide plateau in the Bode plot, ranging from 10^2 Hz to 10^{-2} Hz. The phase angles were roughly unchanged through this whole range. At the initial immersion times there was a small decrease of the phase angles at the lowest frequencies. After a 30 days period this behavior have become less pronounced and the phase angles increased.

Because of the porous nature of the sintered 316L component tested in this work it would be expected that some diffusion related phenomena appeared in the EIS plots. The Nyquist plots would present a capacitive loop followed by a line with a slope of 45º with the real axis in the low frequency region if diffusion controlled impedance, that is, Warburg impedance were controlling the electrochemical behavior. For porous electrodes, according to the de Levie model [13] this value would be 22.5º. None of these features were seen in the Nyquist plots of Fig. 2a, independently of the immersion time. Bautista et al. [14] studied the corrosion resistance of ferritic sintered stainless steels in sodium sulfate solution using EIS measurements and did not found diffusion controlled phenomena for the as-sintered materials. On the other hand, Sobral et al. [15], investigating the corrosion processes of powder injection molded 316L stainless steel in NaCl solution, ascribed a Warburg impedance element to explain EIS measurements results. The results obtained in the present work indicate that the gas atomized 316L component is corrosion resistant in the simulating PEM fuel cell electrolyte. This condition was stable throughout the whole test.

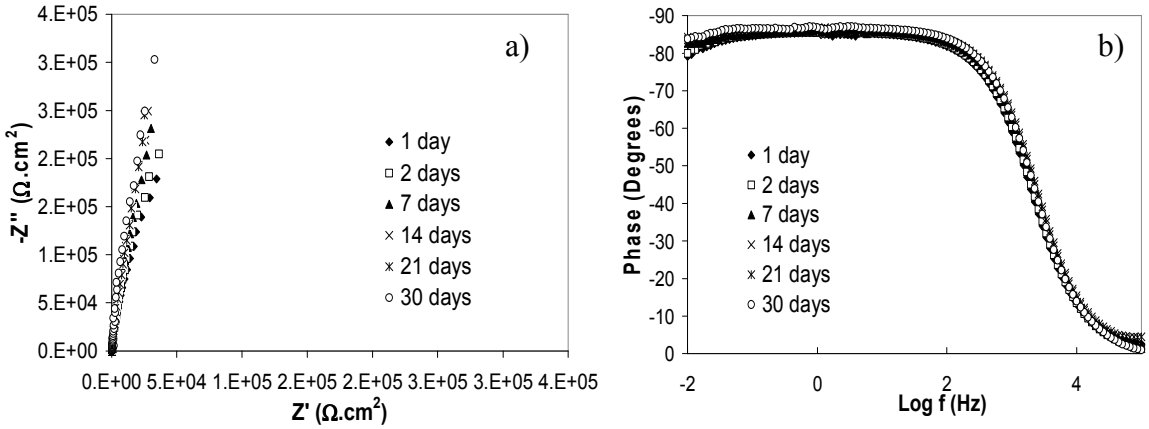

Figure 2. EIS diagrams of PIM 316L specimens after 1, 2, 7, 14, 21 and 30 days of immersion in 0.5 M H_2SO_4 + 2 ppm HF solution at room temperature: (a) Nyquist and (b) Bode plots.

In order to quantify the corrosion effects observed in the EIS plots of Fig. 2 the experimental data were simulated with electrical equivalent circuits (EEC). The fitting procedure was based upon the non-linear least squares method. The circuit that best represented the electrochemical response of PIM 316L is shown in Figure 3. The capacitive behavior was simulated using constant phase elements (CPE) instead of pure capacitors to take into account the non-uniform current distribution along the surface of the electrode.

R_e represents the electrolyte resistance, R_{ox} and C_{ox} are the resistance and the capacitance of the redox transformation of the corrosion products that occurs on the surface of the passive film (first time constant), R_{ct} and C_{dl} are the charge transfer resistance and the double layer capacitance (second time constant). The parameters n_{Cox} and n_{Cdl} are the exponents of the constant phase elements used to simulate the capacitance of the first and second time constants, respectively. The quality of the fitting process may be seen in Fig. 4.

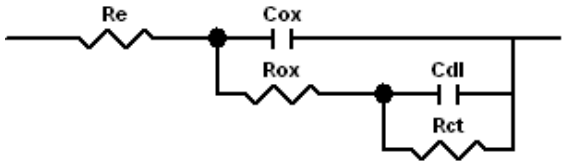

Figure 3. EEC used to simulate the experimental EIS data obtained from PIM 316L stainless steel immersed in 0.5 M H_2SO_4 + 2 ppm HF solution at room temperature.

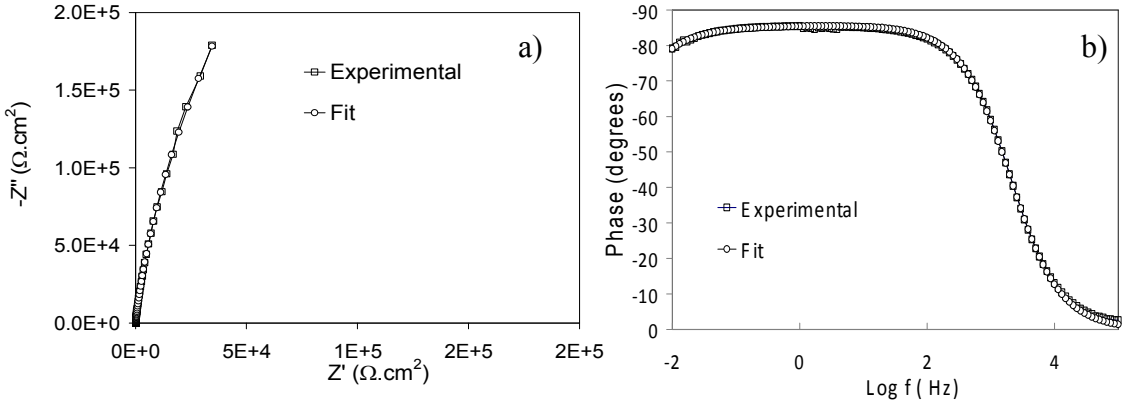

Figure 4. Experimental and fitted data of EIS plots from PIM 316L specimens after 1 day of immersion in 0.5 M H_2SO_4 + 2 ppm HF solution at room temperature: (a) Nyquist and (b) Bode plots.

Only the plots related to 1 day of immersion are presented. The same circuit was suitable to simulate the experimental data from the periods of 2, 7, 14, 21 and 30 days of immersion. From 1 to

30 days no new time constant was necessary to model the electrochemical response of the electrode. This is a strong indication of its stability in the test solution. The values of the electrochemical parameters calculated from the EIS spectra using the EEC of Fig. 3 are shown in Table 2. The low values of R_{ox} for all the immersion periods suggest that the corrosion resistance is determined by R_{ct}. Bautista et al. [14] found a similar tendency for as-sintered ferritic stainless steels. Moreover, R_{ct} values increase with immersion time, confirming the behavior shown in the Nyquist plots of Fig. 2a. The potentiodynamic polarization curve of PIM 316L stainless steel, after 30 days of immersion in 0.5 M H_2SO_4 + 2 ppm HF solution, at room temperature, is shown in Fig. 5. The curve is typical of an active electrochemical behavior. Current density continuously increases with the applied potential. The corrosion current density (i_{corr}) was determined to be 0.4 $\mu A.cm^{-2}$ by extrapolating the anodic Tafel slope up to the corrosion potential (E_{corr}) value. The corrosion potential (E_{corr}) was 0.33 V_{SCE}. The low i_{corr} value indicates that the material presented high corrosion resistance in the electrolyte, confirming EIS results. This behavior strongly suggests that the porosity of the PIM 316L stainless steel was not a critical factor to enhance the corrosive attack during the test.

Table 2. Parameters calculated from the EIS spectra using the EEC of Fig. 3.

Time of immersion (days)	R_e ($\Omega.cm^2$)	C_{ox} ($\mu F.\ cm^{-2}.s^{\alpha-1}$)	n_{Cox}	R_{ox} ($\Omega.cm^2$)	C_{dl} ($\mu Fs^{\alpha-1}cm^{-2}$)	n_{Cdl}	R_{ct} ($M\Omega.cm^2$)
1	1.68	61.6	0.96	24.2	13.5	0.88	1.74
2	1.69	47.7	0.98	24.0	20.6	0.87	2.67
7	1.68	44.4	0.98	23.6	17.2	0.88	3.77
14	1.70	42.7	0.98	23.2	13.8	0.88	5.32
21	1.64	36.4	0.97	22.7	19.9	0.89	5.51
30	1.79	43.0	0.99	26.6	18.9	0.88	5.68

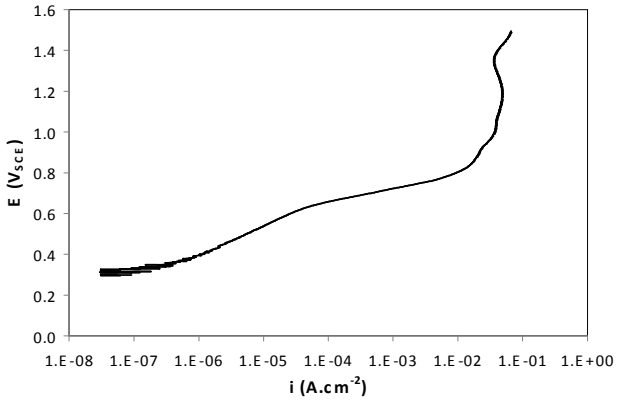

Figure 5. Potentiodynamic polarization curves of PIM 316L stainless steel after 30 days of immersion in 0.5 M H_2SO_4 + 2 ppm HF solution at room temperature.

The surface morphology of the PIM 316L stainless steel is shown in Fig. 6. Two different conditions are presented, i.e. as-received and after the polarization test. The as-received material presents pores coarsening as shown in Fig. 6a. This morphology was also observed by Suri et al. [16] for gas-atomized 316L consolidated particles. After polarization the surface morphology was strongly altered. The pores have diminished as a consequence of the corrosion processes undertaken during 30 days of immersion in the electrolyte. Apparently, the effect of the electrolyte was to promote the formation of a more continuous oxide layer on the stainless steel surface. Small and round pores are present on the materials' surface. This morphology may be the cause of the increase of R_{ct} values with the immersion time as calculated from the EIS spectra of Fig. 2. Furthermore, no pitting has been observed pointing to an active degradation mechanism as shown in the anodic polarization curves of Fig. 5.

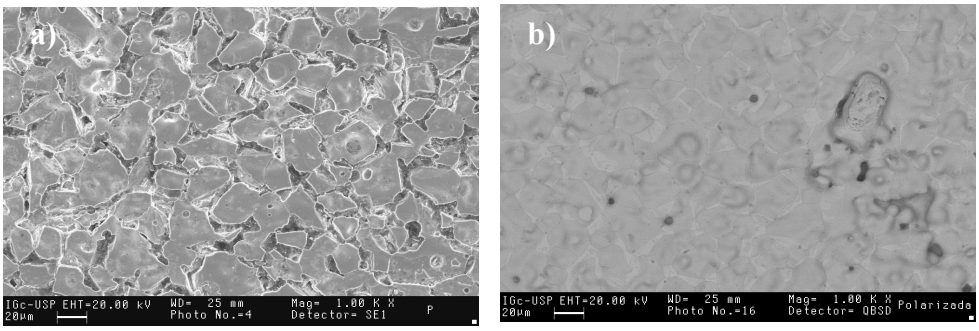

Figure 6. SEM micrographs of PIM 316L stainless steel: (a) as-received (secondary electrons) and (b) after polarization test (backscattered electrons).

Conclusions

PIM 316L stainless steel showed high corrosion resistance in simulated PEM fuel cell electrolyte. The impedance values increased with immersion time indicating the high stability of the material during the test. The blockage of pores, as observed by SEM after polarization test, may account for this behavior. The small mean pore size and low porosity level are key parameters to explain the suitable corrosion behavior observed in the electrochemical tests.

Acknowledgements

The authors are thankful to Electrocell Ind. Com. LTDA, São Paulo, Brazil for providing the infrastructure necessary to carry out the electrochemical measurements of this work.

References

[1] H. Tsuchiya, O. Kobayashi: Int. J. Hydrogen Energy Vol. 29 (2004), p. 985.
[2] H. Tawfik, Y. Hung, D. Mahajan: J. Power Sources Vol. 163 (2007), p. 755.
[3] H. Wang, M. A. Sweikart, J. A.: J. Power Sources Vol. 115 (2003), p. 243.
[4] D. P. Davies, P. L. Adcock, M. Turpin, S. J. Rowen: J. Power Sources Vol. 86 (2000), p. 237.
[5] R. C. Makkus, A. H. H. Janssen, F. A. de Bruijn, R. K. A. M. Mallant: J. Power Sources Vol. 86 (2000), p. 274.
[6] A. K. Iversen: Corros. Sci. Vol. 48 (2006), p. 1036.
[7] M. Kumagai, S.-T. Myung, S. Kuwata, R. Asaishi, H. Yashiro: Electrochim. Acta Vol. 53 (2008), p. 4205.
[8] S.-J. Lee, J.-J. Lai, C.-H. Huang: J. Power Sources Vol. 145 (2005), p. 362.
[9] W. Silveira, M. A. Carvalho, R. Machado, W. Ristow Jr., P. A. P. Wendhausen, P. C. Borges, in: 17 CBECIMAT (Congresso Brasileiro de Engenharia e Ciência dos Materiais) Foz do Iguaçu, Brazil (2006).
[10] E. Otero, A. Pardo, E. Sáenz, M. V. Utrilla, P. Hierro: Corr. Sci. Vol. 38 (1996), p. 1485.
[11] E. Otero, A. Pardo, M. V. Utrilla, F. J. Pérez, C.Merino: Corr. Sci. Vol. 39 (1997), p. 453.
[12] C. Moral, A. Bautista, F. Velasco: Corr. Sci. Vol. 51 (2009), p. 1651.
[13] De Levie, R.: Electrochimica Acta Vol. 8 (1963), p. 751.
[14] A. Bautista, A. González-Centeno, G. Blanco, S. Guzmán: Materials Characterization Vol. 59 (2008), p. 32.
[15] A. V. C. Sobral, W. Ristow Jr., D. S. Azambuja, I. Costa, C. V. Franco: Corr. Sci. Vol. 43 (2001), p. 1019.
[16] P. Suri, R. P. Koseski, R. M. German: Mater. Sci. Eng. A. Vol. 402 (2005), p. 341.

Advanced Powder Technology VII
doi:10.4028/www.scientific.net/MSF.660-661

Investigation on the Corrosion Resistance of PIM 316L Stainless Steel in PEM Fuel Cell Simulated Environment
doi:10.4028/www.scientific.net/MSF.660-661.209